

Summer 2004
UNDERGRADUATE RESEARCH INSTITUTE IN ASTROPHYSICS (URIA)



DETERMINING THE PECULIAR VELOCITY OF GALAXIES FOUND IN SDSS

Wanda Moses

Computer Science/Mathematics Undergraduate, Mathematics and Computer Science
Department, South Carolina University, 300 College Street NE, Orangeburg, SC 29117

Constance Ray

Industrial Engineering Technology, Industrial and Electrical Engineering Technology
Department, South Carolina University, 300 College Street NE, Orangeburg, SC 29117

Jennifer Sanders

Mathematics Education Undergraduate, Mathematics and Computer Science Department,
South Carolina University, 300 College Street NE, Orangeburg, SC 29117

Mentor:

Dr. Daniel M. Smith

Associate Professor of Physics, Physical Sciences Department, South Carolina State
University, 300 College Street NE, Orangeburg, SC 29117

ABSTRACT

We present an analysis of the two-dimensional correlation function, $\xi(r_p, \pi)$, based on the Sloan Digital Sky Survey (SDSS) Data Release 2 (DR2). The sample consists of 118, 887 galaxies, which covers an area of 3324 square degrees. With the data, we plotted $\xi(r_p, \pi)$ to observe the effect of peculiar velocities.

1. INTRODUCTION

The two-point correlation function is a fundamental statistic of the galaxy distribution, and is relatively straightforward to calculate from observational data. In the Sloan Digital Sky Survey (SDSS), 2-degree Field Galaxy Redshift Survey (2dFGRS), and Las Campanas Survey, tens of thousands of galaxies were used to characterize large-scale structure. Zehavi, et. al. (2002) (SDSS), and Hawkins, et. al.(2003) (2dFGRS) have calculated the two-point correlation function. We also calculate the red-shift space and two-dimensional two-point correlation functions using SDSS data but with a much larger number of galaxies than Zehavi2002 (29,300 vs. 103,502).

The next section will give background to SDSS. Section 3 will describe the two-point correlation function. Section 4 will describe the calculation of both the red-shift and the two-dimensional correlation functions. Section 5 will summarize the results.

2. SLOAN DIGITAL SKY SURVEY (SDSS)

The SDSS will map the local universe by acquiring imaging data in five color bands (350-910 nm) down to $m=23$ over π steradians in the northern sky and 0.074π steradians in the southern sky. Spectroscopic data will be acquired for almost a million galaxies. The SDSS telescope is located at Apache Point Observatory in Sunspot, New Mexico. The principal survey goals are to measure the large-scale distribution of galaxies and quasars and to produce an imaging and spectroscopic legacy for the astronomical community. We use the latest data from DR2. This data is located at <http://www.sdss.org/DR2> and lets the users download information from the Catalog Archive Server (CAS).

3. TWO-POINT CORRELATION FUNCTION

The two-point correlation function $\xi(r)$ has been the primary tool for calculating large-scale cosmic structure. The probability of finding a galaxy in each of the volume elements dV_1 and dV_2 separated by the distance r

$$dP_1 dP_2 = \frac{dV_1}{V} \frac{dV_2}{V} (1 + \xi(r)).$$

Suppose N points are distributed in a volume V . The density is then $n=N/V$. If the points are randomly distributed in the sky then the probability that a given point has a neighbor in a surrounding volume dV is $dP=n dV$. However, if there is some clustering of the galaxies then $dP=n dV [1+\xi(r)]$, where r is the distance from the first point and $\xi(r)$ is the two-point correlation function. If the points are correlated, i.e. they are clustered, then $\xi(r)>0$. Alternatively, we can define a value r_0 within which the clustering will be $\xi(r)>1$. In essence, the two-point correlation function, $\xi(r)$, is the probability above random that one galaxy is at a distance r away from another galaxy.

The redshift-space correlation function, $\xi(s)$ differs from the real-space correlation function, $\xi(r)$ because of peculiar velocities. Redshift space distortions can be corrected by computing the correlation function $\xi(r_p, \pi)$, where a pair of galaxies with

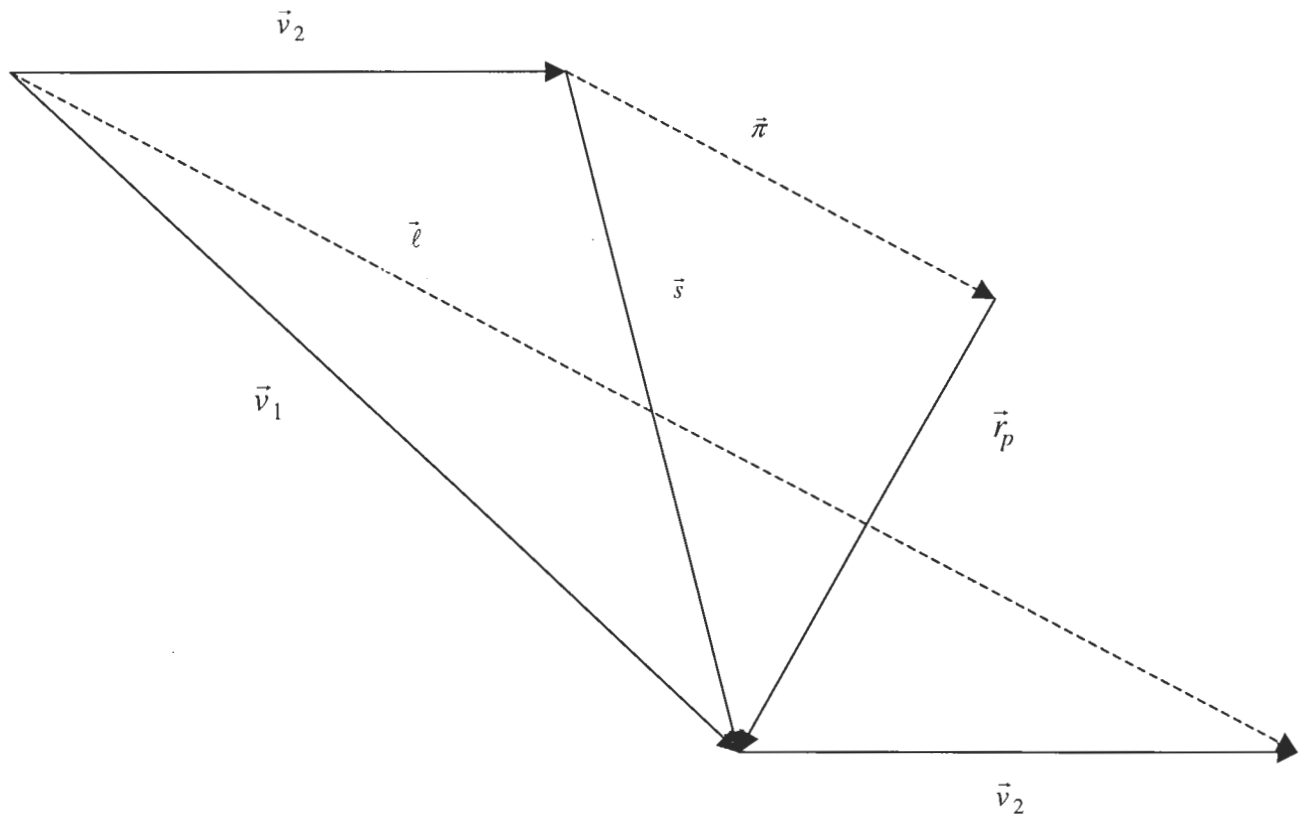


Fig. 1-Vector diagram of peculiar velocity differences, \vec{r}_p (infall) and $\vec{\pi}$ (line-of-sight).

red-shift positions v_1 and v_2 , can define the red-shift separation vector $\vec{s} \equiv \vec{v}_1 - \vec{v}_2$ and the line-of-sight vector $\vec{\ell} \equiv \frac{1}{2}(\vec{v}_1 + \vec{v}_2)$ (Fig.1).

4. DATA ANALYSIS

We gather galaxy data from the SDSS DR2 catalog. We read the data into a *Mathematica* program to plot the large-scale structure of the universe. We make two- and three-dimensional plots. We calculate and plot the red-shift space correlation function using previously developed programs. We also present a graph of our two-dimensional correlation function calculation. We do not account for systematic errors.

4.1 Large-Scale Structure of the Universe

The measurements of redshift (z) and right ascension (ra) are used to produce two-dimensional polar plots (Figs. 2 & 3). The two-dimensional polar plots are created using 34,970 galaxies. Fig. 2 is created to show the large-scale structure for the actual galaxies. It helps to further prove that gravity causes clustering, and it shows filaments and voids. Fig. 3 is a random distribution of 34,970 galaxies where there are no filaments, voids or clustering. Figs. 2 & 3 show a thin slice through the universe with the

Milky Way galaxy situated at the narrow end of the slice. In order to create the two-dimensional polar plots in red-shift space, we use the parameters

$$-3^\circ < \text{dec} < 3^\circ,$$

$$0^\circ < \text{ra} < 360^\circ,$$

$$z < 0.1.$$

We use the measurements that are taken for the red-shift, right ascension, and declination (*dec*) of 103,502 galaxies to generate a three-dimensional plot for the actual and random galaxies in the red-shift space. The graphical representation of these galaxies is achieved by translating the red-shift into the comoving distance (D_c) using the equation:

$$D_c = D_H \int_0^z \frac{1}{\sqrt{\Omega_M (1+z)^3 + \Omega_k (1+z)^2 + \Omega_\Lambda}} dz,$$

where $\Omega_k = 0$, $\Omega_\Lambda = 0.73$, and D_H is the Hubble Distance, which is the speed of light c multiplied by the Hubble time: $D_H = 3000 h^{-1} \text{ Mpc}$, (Hogg, 2000).

When we use the comoving distance with the *ra* and *dec* angle values, we are able to generate the Cartesian co-ordinates, x_c , y_c , and z_c . We transform the data to Cartesian co-ordinates by using the equations:

$$x_c = D_c(z) \text{Sin}(90^\circ - \text{dec}) \text{Cos}(\text{ra}),$$

$$y_c = D_c(z) \text{Sin}(90^\circ - \text{dec}) \text{Sin}(\text{ra}),$$

$$z_c = D_c(z) \text{Cos}(90^\circ - \text{dec}).$$

Fig. 4 consists of 103, 502 galaxies with red-shift, apparent magnitude, and absolute magnitude restrictions (see below), illustrating the large-scale structure of the universe. Fig. 4 illustrates that the galaxies are not uniformly distributed. In contrast, Fig. 5 illustrates how a random distribution of 103,502 galaxies would appear. We create the three-dimensional plots in red-shift space by using the parameters:

$$-90^\circ < \text{dec} < 90^\circ,$$

$$0^\circ < \text{ra} < 360^\circ,$$

$$0.019 < z < 0.13.$$

4.2 Analysis of the Two-Point Correlation Function

We downloaded data for 118,887 galaxies from the SDSS DR2 catalog. However, we restrict the data range from which the galaxy data is taken. The flux limit of r in the spectroscopic survey is 22.2. In our work, we limit our sample to a range in red-shift of $0.019 < z < 0.13$, a bright and faint apparent magnitude of $14.5 < m < 17.6$, and a selected absolute magnitude range of $-22 < M < -19$ (Zehavi 2002). The reason for Zehavi's z limits is to make systematic error corrections simpler, and the M limits extract the brightest galaxies without generating interference between spectra. The red-shift, the apparent magnitude, and the absolute magnitude restrictions reduce the number of galaxies from 118,887 to 103,502.

We use the following equation to find the absolute magnitude:

$$M = m - D_M(z) - K(z),$$

where M is the absolute magnitude, m is the apparent magnitude, $D_M(z)$ is the distance modulus and $K(z)$ is the K-correction (Zehavi 2002). The comoving distance (D_c) depends on the cosmology assumed. In order to calculate the D_c , we use the standard formula tabulated by Hogg, (2000), noted above, while assuming a uniform Hubble flow.

Our data comes from examining galaxies at a fixed observed wavelength band. For our calculations, we estimate the K-correction using

$$K(z) = 2.5 \log_{10} (1 + z).$$

Lin, et. al. (1996) states that it is appropriate to use that K-correction formula for the mean of an r-band selected galaxy sample.

The data, with the restrictions and the K-corrections, are used in a C++ program to calculate the distance between every pair of galaxies. They are assigned to bins, which are $1 h^{-1} Mpc$ in length. After the distances are calculated and assigned to bins, we calculate the red-shift space correlation function, $\xi(s)$ (Fig 6). In order to calculate the correlation function, we use the procedure described by Groth, et. al. (1977):

$$\xi(r) = \left(\frac{\text{Number of Pairs of Galaxies at } r}{\text{Number of Random Pairs of Galaxies at } r} \right) - 1.$$

We observe the same slope as Zehavi but a different amplitude, likely due to our omission of systematic error corrections described below.

For the two-dimensional correlation function, $\xi(r_p, \pi)$, we use the distances between the pairs of galaxies to calculate $\pi \equiv \vec{s} \cdot \vec{l} / |\vec{l}|$ and $r_p (r_p^2 \equiv s^2 - \pi^2)$, which are assigned to two-dimensional bins. The procedure is the same as indicated for $\xi(r)$ above. In Figs. 7 & 8 are graphs of the results from the two-point correlation function. In Fig 7, the graph shows the effects of peculiar velocities in relationship π and r_p with a peak located at $r_p = 0$. This means that the velocity differences are along the line-of-sight. When r_p moves away from zero, the dark matter is attracting the galaxies, which is indicated on the plot by the decrease of the $\bar{\pi}$ component of \vec{s} . However, Fig. 8 has an irregularity as r_p approaches 0.

4.3 Systematic Errors in Analysis

There are two types of systematic errors that should be considered when analyzing peculiar velocities of galaxies. One is the unaccounted for bright galaxies. The other error is due to two galaxies being too close together, where both of them cannot be accounted for in the red-shift measurements.

5. SUMMARY

We use SDSS DR2 catalog to extract data for 118,887 galaxies. We restrict the analysis to red absolute magnitude, $-22 < M_r < -19$ and $0.019 < z < 0.13$, leaving us with 103,502 galaxies. We make two-dimensional polar plots, and three-dimensional plots of galaxy positions. We also plot the red-shift space correlation function, and a contour plot of the two-dimensional correlation function. Our red-shift space correlation function is similar to those calculated by others. Our contour plot clearly shows the peculiar velocities due to small-scale gravitational attraction and larger-scale infall of galaxies due to dark matter.

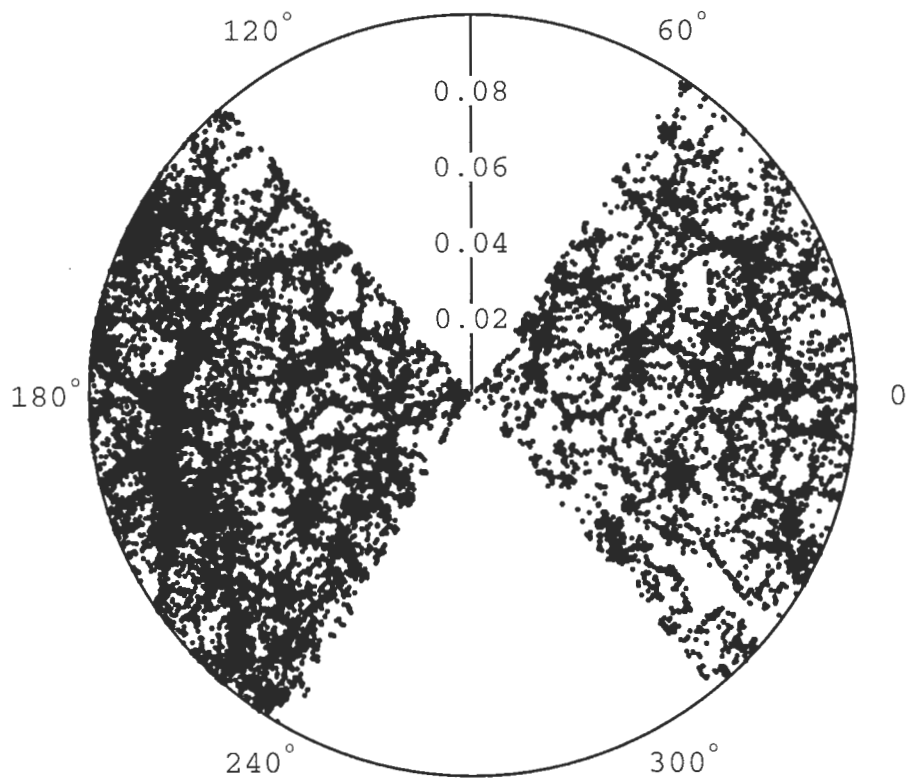


Fig. 2 – Equatorial 2D Polar Plot of 34,970 galaxies in redshift space. The galaxies lie within $|\delta| < 3^\circ$ of the Celestial Equator.

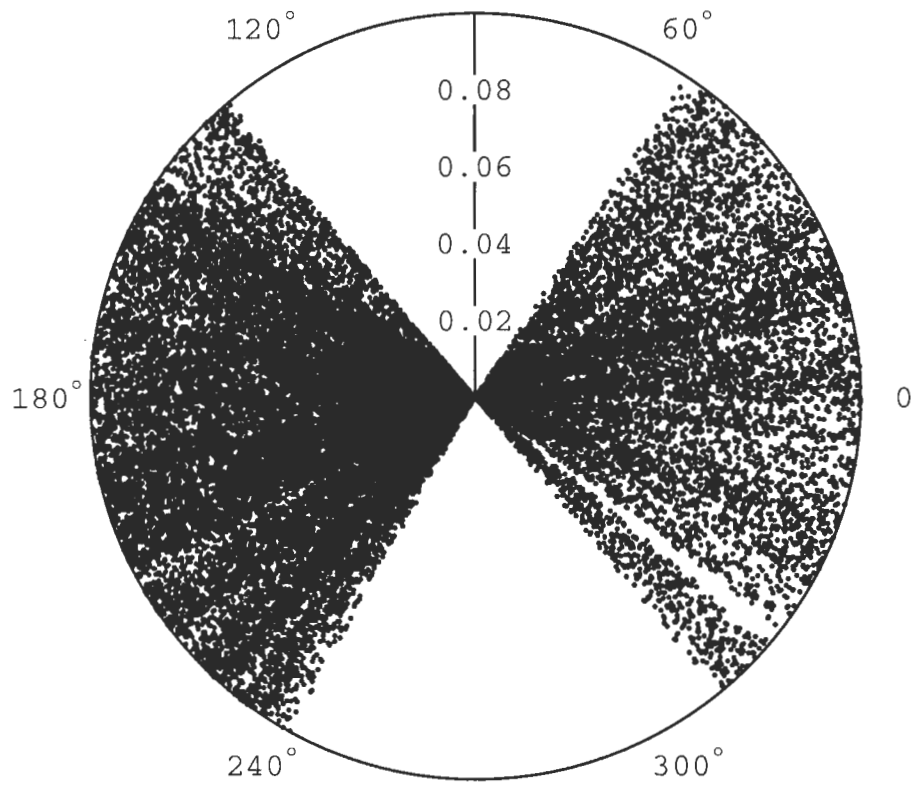


Fig. 3 –Equatorial 2D Polar Plot of 34,970 random galaxies in redshift space. The galaxies lie within $|\delta| < 3^\circ$ of the Celestial Equator.

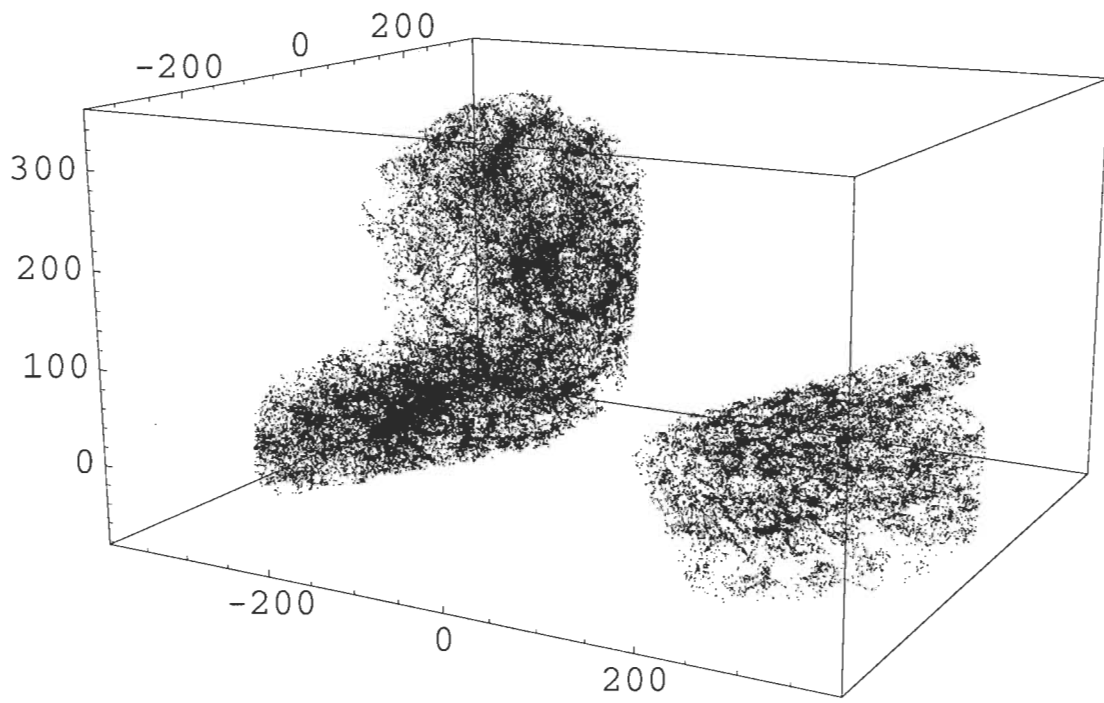


Fig. 4 - 3D Plot of 103,502 Galaxies. The measurements are $h^{-1} Mpc$.
 $-90^\circ < \text{dec} < 90^\circ$

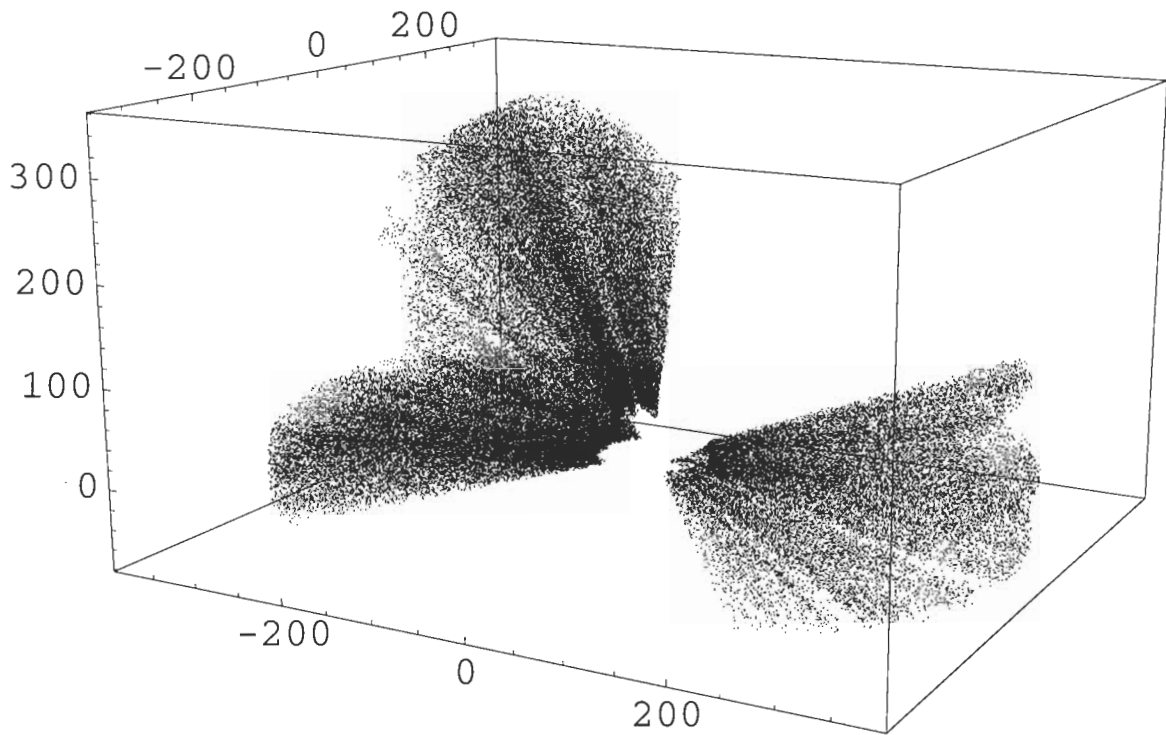


Fig. 5 - 3D Plot of 103,502 Random Galaxies. The measurements are $h^{-1} Mpc$.
 $-90^\circ < \text{dec} < 90^\circ$

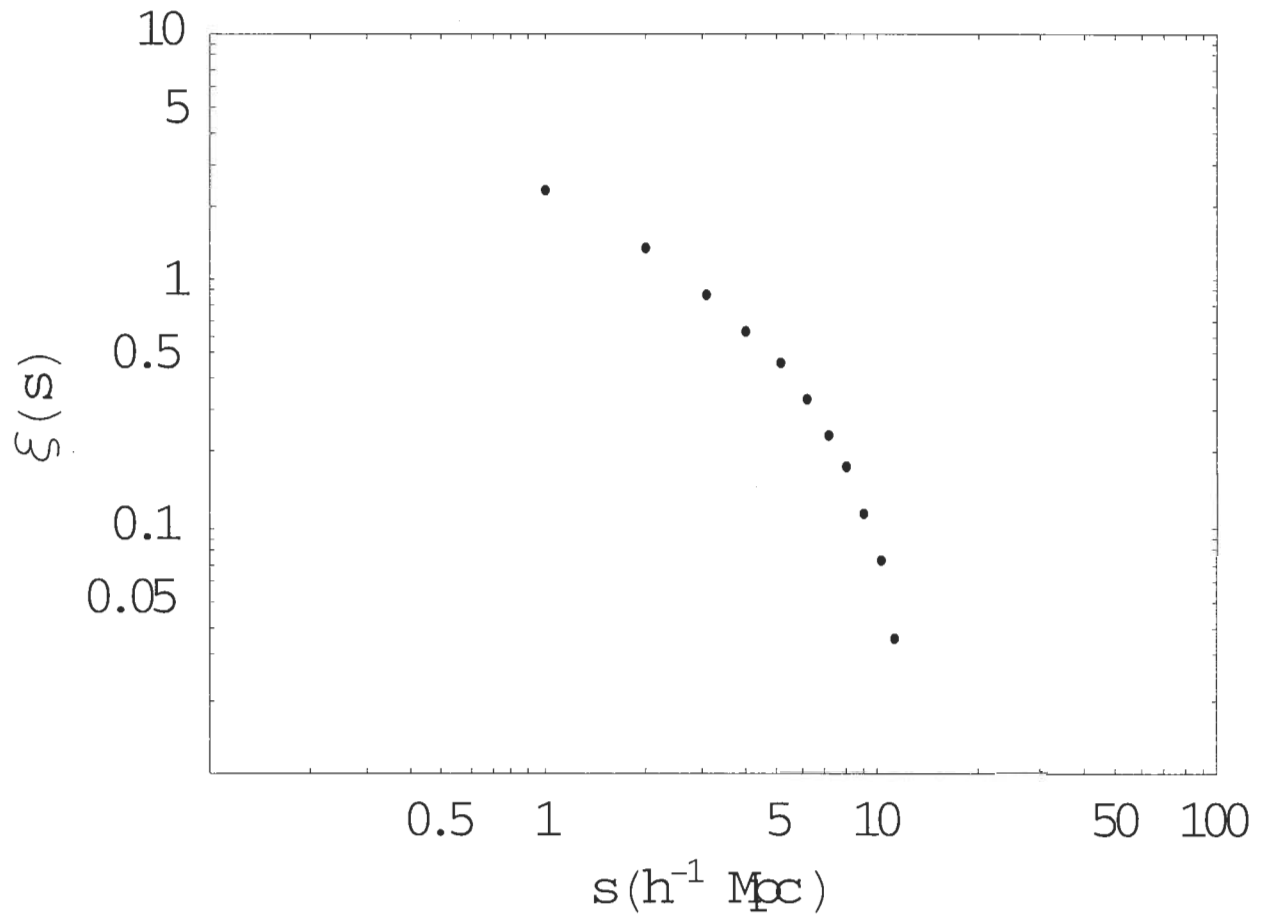


Fig. 6 – Redshift-space correlation function for 103,502 galaxies.

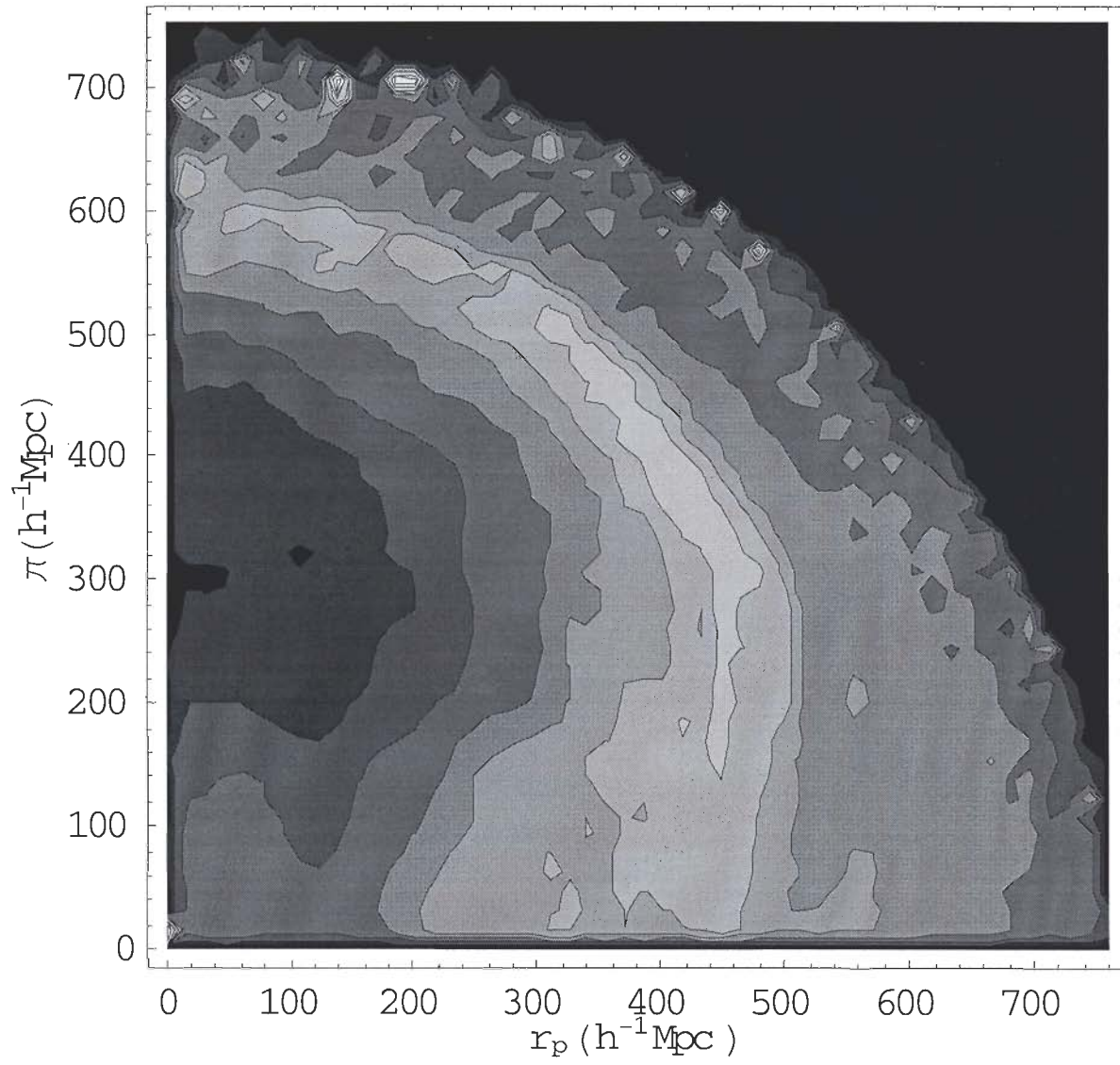


Fig. 7– Contour plot of the correlation function of $\xi(r_p)$.

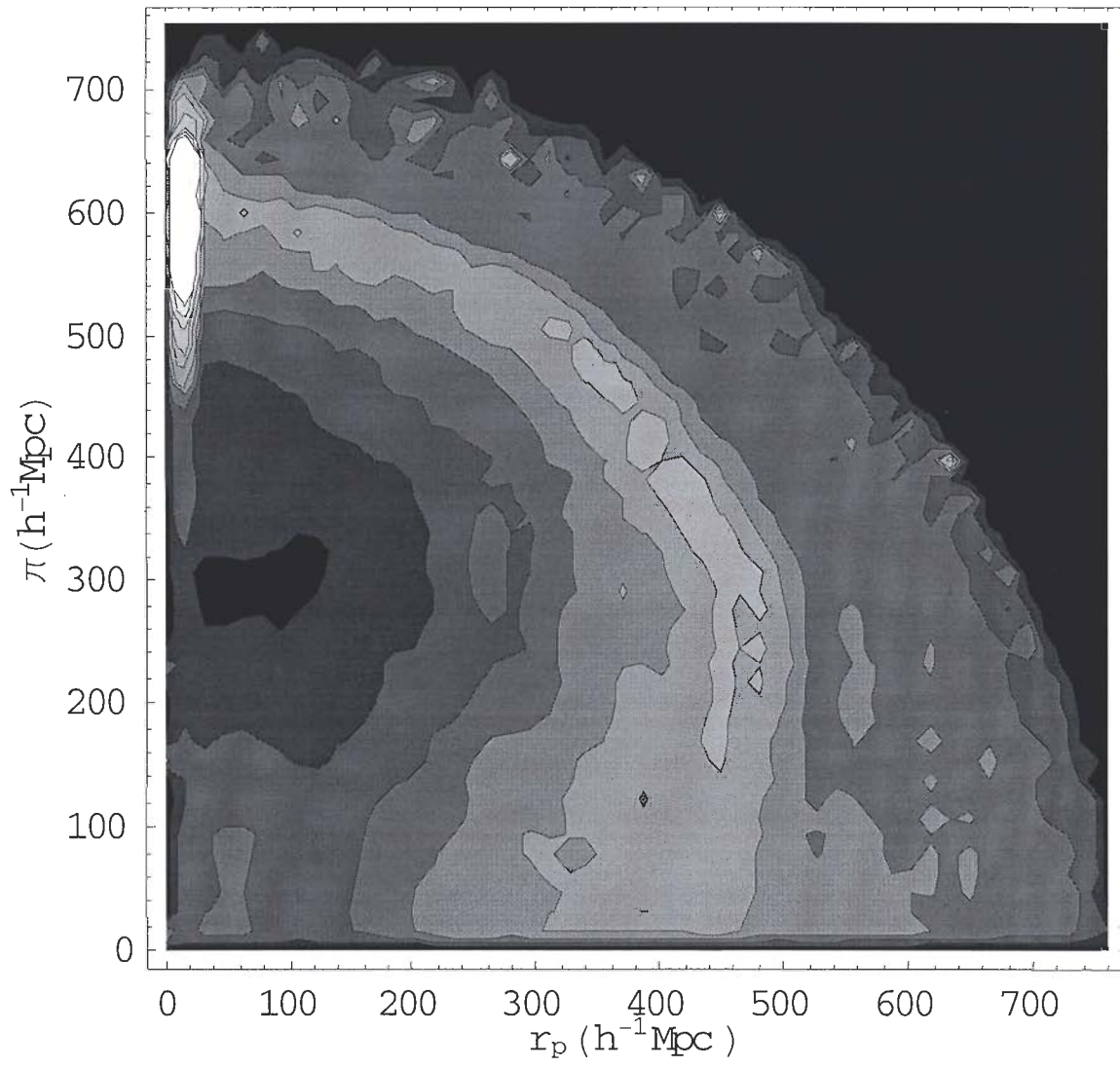


Fig. 8– Contour plot of the correlation function of $\xi(r_p)$.

REFERENCES

- Davis, M., & Peebles, P. J. E. 1983, ApJ, 208, 13
- Groth, E.J., Peebles, P.J.E., Seldner, M., Soneira, R.M. 1977, SciAm 237, p. 76-78, 84, 87-90
- Hawkins, E, et al. 2003, Mon. Not. Astron. Soc. 00,1-19 (2003), 2
- Hogg, D.W. 2000, astro-ph/9905116
- Jing, Y.p., Borner, G., & Suto, Y. 2001, astro-ph/0104023
- Lin, H., et al. 1996, astro-ph/9602064
- Marzke, R.O., et al. 1995, AJ, 110, 477
- Munoz, J.A., et al. 2003, URIA 2003 (SCSU) unpublished, 3,14
- Peacock, J.A., et al.2001, Nature, 410,169
- Shectman, S. A., et al. 1996, astro-ph/9604167
- Zehavi, I., et al. 2002, The SDSS Collaboration, ApJ, 571, 172
- Sloan Digital Sky Survey, http://physics.scsu.edu/~dms/cosmology/LSS_Lab.html